NeuroImage 78 (2013) 186–195

Contents lists available at SciVerse ScienceDirect

NeuroImage

journal homepage: www.elsevier.com/locate/ynimg

fMRI in the awake marmoset: Somatosensory-evoked responses, functional connectivity, and comparison with propofol anesthesia

Junjie V. Liu [a,1], Yoshiyuki Hirano [a,2], George C. Nascimento [a,3], Bojana Stefanovic [a,4], David A. Leopold [b,c], Afonso C. Silva [a,*]

[a] Cerebral Microcirculation Unit, Laboratory of Functional and Molecular Imaging, National Institute of Neurological Disorders and Stroke, National Institutes of Health, 10 Center Drive, Building 10, Room B1D106, Bethesda, MD 20892, USA
[b] Section on Cognitive Neurophysiology and Imaging, Laboratory of Neuropsychology, National Institute of Mental Health, National Institutes of Health, 49 Convent Dr., Building 49 Room 1E21, Bethesda, MD 20892, USA
[c] Neurophysiology Imaging Facility, National Institute of Mental Health, National Institute of Neurological Disorders and Stroke, National Eye Institute, National Institutes of Health, 49 Convent Dr., Building 49 Room 1E21, Bethesda, MD 20892, USA

ARTICLE INFO

Article history:
Accepted 14 March 2013
Available online 6 April 2013

Keywords:
Awake non-human primate
Functional MRI
New world monkey
Neuroanesthesia
Resting-state functional connectivity

ABSTRACT

Functional neuroimaging in animal models is essential for understanding the principles of neurovascular coupling and the physiological basis of fMRI signals that are widely used to study sensory and cognitive processing in the human brain. While hemodynamic responses to sensory stimuli have been characterized in humans, animal studies are able to combine very high resolution imaging with invasive measurements and pharmacological manipulation. To date, most high-resolution studies of neurovascular coupling in small animals have been carried out in anesthetized rodents. Here we report fMRI experiments in conscious, awake common marmosets (*Callithrix jacchus*), and compare responses to animals anesthetized with propofol. In conscious marmosets, robust BOLD fMRI responses to somatosensory stimulation of the forearm were found in contralateral and ipsilateral regions of the thalamus, primary (SI) and secondary (SII) somatosensory cortex, and the caudate nucleus. These responses were markedly stronger than those in anesthetized marmosets and showed a monotonic increase in the amplitude of the BOLD response with stimulus frequency. On the other hand, anesthesia significantly attenuated responses in thalamus, SI and SII, and abolished responses in caudate and ipsilateral SI. Moreover, anesthesia influenced several other aspects of the fMRI responses, including the shape of the hemodynamic response function and the interareal (SI–SII) spontaneous functional connectivity. Together, these findings demonstrate the value of the conscious, awake marmoset model for studying physiological responses in the somatosensory pathway, in the absence of anesthesia, so that the data can be compared most directly to fMRI in conscious humans.

Published by Elsevier Inc.

Introduction

Since its inception 20 years ago (Ogawa et al., 1992), functional magnetic resonance imaging (fMRI) has established itself as the most prominent tool in brain research — for a review, see Bandettini (2012). The physiological basis of fMRI relies on a tight relationship between neural activity and local regulation of cerebral blood flow (CBF), volume (CBV) and oxygen consumption (CMRO2) (Attwell and Iadecola, 2002). Yet, in spite of the widespread use of fMRI to study brain function, the underlying fMRI signal mechanism and its functional specificity are still to be fully elucidated (Logothetis, 2008).

The use of animal models has been fundamental not only to the development of fMRI techniques, but also to provide a better understanding of the underlying mechanisms of functional brain activation — for reviews see Silva et al. (2011) and Van der Linden et al. (2007). In particular, due to their close phylogeny to humans, nonhuman primates have provided crucial insight into the mechanisms of sensory perception (Dubowitz et al., 2001; Lipton et al., 2006; Maier et al., 2008; Petkov et al., 2006; Schmid et al., 2010; Srihasam et al., 2010; Wilke et al., 2009) and brain cognition (Nakahara et al., 2002; Nelissen and Vanduffel, 2011). To date, old world macaques have been the subjects of the vast majority of fMRI studies in non-human primates (Andersen et al., 2002; Gamlin et al., 2006; Goense et al., 2010; Joseph

* Corresponding author. Fax: +1 301 480 2558.
E-mail addresses: liu@junjie.com (J.V. Liu), hirano@chiba-u.jp (Y. Hirano), georgegcn@gmail.com (G.C. Nascimento), bojana@sri.utoronto.ca (B. Stefanovic), SilvaA@ninds.nih.gov (A.C. Silva).
[1] Current address: c/o Office of Student Affairs, Geisel School of Medicine at Dartmouth, 302 Remsen, Hanover NH 03755, USA.
[2] Current address: Research Center for Child Mental Development, Chiba University Graduate School of Medicine. 1-8-1 Inohana, Chuo-ku, Chiba 260-8670, Japan. Fax: +81 43 226 8588.
[3] Current address: Dept. of Biomedical Engineering, Federal University of Rio Grande do Norte. Av. Senador Salgado Filho S/N Lagoa Nova 59075-000, Natal, Brazil.
[4] Current address: Dept. of Medical Biophysics, Sunnybrook Health Sciences Centre, University of Toronto. 2075 Bayview Avenue, S-Wing, Suite S6 50 Toronto, ON M4N 3M5, Canada.

1053-8119/$ – see front matter. Published by Elsevier Inc.
http://dx.doi.org/10.1016/j.neuroimage.2013.03.038

et al., 2006; Keliris et al., 2007; Logothetis et al., 1999; Murnane and Howell, 2010; Pfeuffer et al., 2007). However, New World monkeys, such as common marmosets (*Callithrix jacchus*), are becoming increasingly popular due to their practical advantages, such as small size, ease of breeding in captivity, short gestation period, short age to sexual maturity and long lifespan (Mansfield, 2003).

Marmosets are comparable in size to rats, and yet their brain size is approximately eight times larger than the rat brain (Marshall and Ridley, 2003). The gyrification of the marmoset brain differs from that of other primates in that they have a highly lissencephalic cortex (Newman et al., 2009). In many ways, these are desirable features for a primate model. First, their size permits high-resolution MRI scanning in state-of-the-art small animal scanners (Bock et al., 2009, 2011). Second, their flat cortex provides a straightforward layout of functionally defined areas on the surface of the brain for study with electrophysiological and optical imaging. Importantly, despite its flatness, the topological layout of areas over the marmoset cortex closely matches that of other primates, including humans. Histological and electrophysiological boundaries, along with anatomical connections, have been charted for many cortical areas, with the structures of visual (Bourne and Rosa, 2006), auditory (Bendor and Wang, 2005; de la Mothe et al., 2006, 2012a,b; Philibert et al., 2005), and somatosensory cortices (Griffin et al., 2010; Krubitzer and Kaas, 1990), showing remarkable similarity to that found in the long studied rhesus macaque.

Neurophysiological studies in animals often use anesthetic agents to maximize experimental control, which can strongly influence brain function. While many aspects of stimulus processing survive in the unconscious animal, the amplitude and spatiotemporal characteristics of the sensory responses depend strongly on the type and concentration of anesthetic. In fMRI experiments, where neural activity is assessed through hemodynamic changes, further complication arises due to the direct effect of the anesthetic on vasculature. Thus, in considering the marmoset as a primate model to study mechanisms of neurovascular coupling and other fMRI-based questions, there is great value in developing a conscious preparation so that physiological responses can be compared most directly to fMRI in conscious humans. Furthermore, in the comparison between anesthetized and awake preparations, the marmoset offers the opportunity to examine the neural effects of anesthesia directly in a nonhuman primate (Mhuircheartaigh et al., 2010).

In the present work, we describe the first fMRI experiments with somatosensory stimulation in the conscious marmoset. The animals were immobilized using a custom-fit head-holder individually tailored for each animal as described previously (Silva et al., 2011). They were acclimated to the scanning sessions with a short but systematic training procedure using video monitoring and positive reinforcement. We measured fMRI responses during awake testing, focusing on BOLD responses to somatosensory stimulation of the forelimb. Cortical and subcortical responses in conscious animals were compared with responses in animals under two anesthetic regimens, presenting a range of stimulation frequencies in all cases. In addition, the coherence in spontaneous BOLD fluctuations, commonly termed functional connectivity, was compared between the conscious and anesthetized animals. We demonstrate that not only is the awake marmoset a viable preparation for state-of-the-art MR scanning, but also that this model poses distinct translational advantages over the anesthetized preparation, since fundamental aspects of the stimulus-evoked response and the functional connectivity are profoundly altered by anesthesia.

Materials and methods

All animal procedures were approved by the National Institute of Neurological Disorders and Stroke (NINDS) and National Institute on Deafness and Other Communication Disorders (NIDCD) Animal Care and Use Committee. Adult common marmosets (*C. jacchus*) were housed in pairs of the same gender two to in cages with a twelve-hour light/dark cycle and ad libitum diet of Zupreem canned marmoset food, Purina 5040 biscuits, unfiltered water, P.R.A.N.G. rehydrator, and fruit and vegetable treats.

Conscious, awake marmosets

Six male marmosets were used for awake fMRI. They were acclimated to being restrained according to the three-week acclimatization schedule procedures described in Silva et al. (2011). Briefly, during the first week, animals were placed in the prone (sphinx) position in an MRI-compatible cradle and acclimated to having their bodies contained for incremental periods of time. During the second week, the acclimatization continued by allowing the animals to hear MRI sounds during incremental periods of body containment. During the third, final week of acclimatization, the animals had their head restrained. Two different techniques were used to restrain the head of the animals. For old marmosets ($n = 3$; age: 7–8 yr), the head was secured by two MR-compatible head posts, which were surgically implanted at the end of the 2nd week of acclimatization under isoflurane anesthesia (2–4%). The animals were allowed to fully recuperate from surgery for 1 week prior to resuming acclimatization to the head restraint. For young marmosets ($n = 3$; age: 1–2 yr), no head implants were used. Instead, individual custom-built helmets were designed for each animal (Silva et al., 2011) based on a 3D contour of each animal's head obtained from a previously acquired 3D gradient-echo MRI dataset of the entire head and neck of the animal. The helmet consisted of a bottom plastic piece to support the chin of the animal and of a top piece to support the head and prevent motion. To provide greater comfort for the animals, 3-mm thick foam was glued onto the inside surface of both top and bottom pieces. Proper and perfect fitting of the pieces to each animal was guaranteed by design, since the shape of each animal's head was used to produce each helmet, assuring comfortable and adequate immobilization.

Anesthetized marmosets

Twelve other marmosets (9 males; age: 2–9 yr) were used for anesthetized fMRI. The animals were fasted 12–16 h prior to the fMRI experiments. On the day of the experiment, the animals were retrieved from their cages and transported to the MRI laboratory. Initial sedation was induced by a small dose of ketamine (4 mg/kg, intramuscular) and isoflurane (2%) inhaled via a facemask. These administrations occurred at least 1.5 h before fMRI started to ensure minimal impact on the functional responses during fMRI acquisitions. After the animal received oral–tracheal intubation and cannulation of a lateral tail vein, it was artificially ventilated with O_2-enriched (30%) air, isoflurane was discontinued and anesthesia was switched to a constant intravenous infusion of either one of the two protocols below:

1) Low-propofol + fentanyl (Low-P): propofol (0.3 mg/kg/min) + fentanyl (10–20 μg/kg/h).
2) High-propofol (High-P): propofol (0.6–1.0 mg/kg/min).

Note that fentanyl, an opioid analgesic agent, was added in order to allow a low dose of propofol to be used to maintain adequate balanced anesthesia in protocol 1, but was not needed when the propofol dose was high (protocol 2). At the beginning of each session, the infusion rates were adjusted within the ranges shown above for each animal at the level necessary to achieve animal immobility. The rates then remained constant throughout the remainder of the experiments (~6 h). The animals were positioned in the prone (sphinx) position in the MRI-compatible cradle with its head secured by ear bars. End-tidal CO_2, pulse oximetry, heart rate and rectal temperature were maintained within normal ranges, and were not systematically different between the two anesthesia regimes (see Inline Supplementary Table S1). At the end of the experiments, infusion of the anesthetics was discontinued and all animals recovered

consciousness within 15 min. They were observed for another 30 min and returned to their home cages.

Inline Supplementary Table S1 can be found online at http://dx.doi.org/10.1016/j.neuroimage.2013.03.038.

Functional MRI

All fMRI measurements were performed in a 7 T/30 cm horizontal magnet interfaced to an AVANCE AVIII MRI spectrometer (Biospec, Bruker Corp., Billerica, MA), and equipped with a 15 cm gradient set capable of generating 450 mT/m within 150 μs (Resonance Research Inc., Billerica, MA, USA). A two-element receive-only surface coil array (inner diam.: 1.6 cm) was positioned on top of the head and near the somatosensory cortex, and actively decoupled from a 12 cm birdcage transmit-only volume coil. Local B_0 inhomogeneity estimation and shimming were performed based on field map measurements. BOLD-weighted echo-planar imaging (EPI) data were acquired in 16 coronal slices (thickness: 0.75 mm; field-of-view: 40 × 36 mm; matrix: 80 × 72; TR: 2 s; TE: 20 ms; 1-shot gradient-echo). To prescribe the slices consistently across sessions, we used anatomical landmarks including the anterior and posterior commissures (AC and PC) in the median plane of brain, which were identified from a single sagittal slice (thickness: 1 mm) acquired with a 2D RARE sequence (Fig. 1). The 16 slices were prescribed orthogonal to the line connecting AC and PC, with the center of slices at 1.875 mm posterior to AC, such that AC was seen in the 11th slice (Fig. 1).

Somatosensory stimulation

During EPI scans, one forearm of each animal was electrically stimulated to measure the evoked fMRI responses. A pair of contact electrode pads (EL258RT, Biopac Systems, Goleta, CA) was placed across the distal end of one shaved forearm; each pad was in tight contact with the skin on the anterior or the posterior side of the forearm to stimulate the median nerve. The pads were connected to a multichannel stimulator (World Precision Instruments, Sarasota, FL), which delivered electrical pulses with fixed width (0.40 ms) and current intensity (1.5 mA for awake and Low-P anesthetized sessions, or 3.0 mA for High-P anesthetized sessions).

In each stimulus trial (40 s), electrical stimulation pulses were presented at a single repetition frequency for 4 s, flanked by a pre-stimulation (6 s) and a post-stimulation (30 s) period. In each scan (800 s), ten different pulse repetition frequencies (1, 2, 4, 6.4, 10, 15.6, 25, 40, 62.5, 125 Hz) were applied twice in a pseudo-randomized order. This design avoids possible habituation effects from repetitively stimulating at one frequency. Approximately 6–8 scans were run in each awake session, and 12–16 scans in each anesthetized session. The timing of stimulus presentation was controlled by Presentation software (Neurobehavioral Systems, Albany, CA). In addition, to measure spontaneous functional connectivity, a few (1–3 per animal) EPI scans (each 800 s long) without stimuli were conducted in each fMRI session.

Data pre-processing

All fMRI data were processed to remove motion artifacts and baseline drifts before further analysis. First, 3D rigid-body motion was estimated and corrected TR-to-TR and scan-to-scan to co-register all volumes in a session. To minimize impact of low spatial frequency artifacts on motion estimation, each 2D slice image was normalized using a homomorphic method (Ress et al., 2007), which comprised three steps: (1) applying a low-pass Gaussian filter (FWHM: 2.5 mm), (2) adding a constant value to both original and filtered images, and (3) dividing the original image by the low-pass filtered image. Motion was estimated from the homomorphic normalized volume, but motion correction was applied to the original data. Next, each 2D slice image was slightly blurred by a low-pass Gaussian filter (FWHM: 0.60 mm) to reduce noise and bring the effective resolution to 0.75 mm (isotropic). Finally, baseline drifts in time series of each voxel were removed by subtracting polynomial fits up to the 2nd order. These pre-processing steps were done using mrVista software (http://white.stanford.edu/software/) and custom code written in MATLAB (MathWorks, Natick, MI, USA).

Stimulus-evoked response: map, regions and amplitude

Statistical significance of stimulus-evoked response was analyzed for each scan with stimulation on a voxel-by-voxel basis. The time series data of each voxel were split into segments, each 40 s long and synchronized to the beginning of each stimulus trial. Each segment was then transformed into the percent signal change from the baseline, defined as the mean signal in the 6 s (4 TRs) pre-stimulus period in each trial. Next, the normalized percentile time series segments of all trials were pooled together for analysis of variance (ANOVA). An F-value was calculated for each voxel to denote the statistical significance of a time series synchronized to the stimulus trial. The F-value was corresponded to the more commonly used statistical P-value by analyzing time series segments that were randomly drawn from data rather than synchronized with stimulus trials (Clare et al., 1999). One advantage of the F-value metric is that it detects both positive and negative responses without a priori assumption of the time course of response.

From previous studies and atlases, we estimated the anatomical boundaries of the upper limb representations in SI and SII, and of the ventroposterior nuclei of thalamus, which carry most thalamocortical projections to SI (Krubitzer and Kaas, 1990; Palazzi and Bordier, 2008; Zhang et al., 2001a,b), as well as the boundaries of the caudate nucleus (Roberts et al., 2007). Regions for further analysis were demarcated using two different methods. The significance-defined regions comprised 64 voxels of the highest F-values within each anatomical boundary. SI and SII regions defined in this way varied in shape but centered on same locations across sessions. These locations could also be predicted

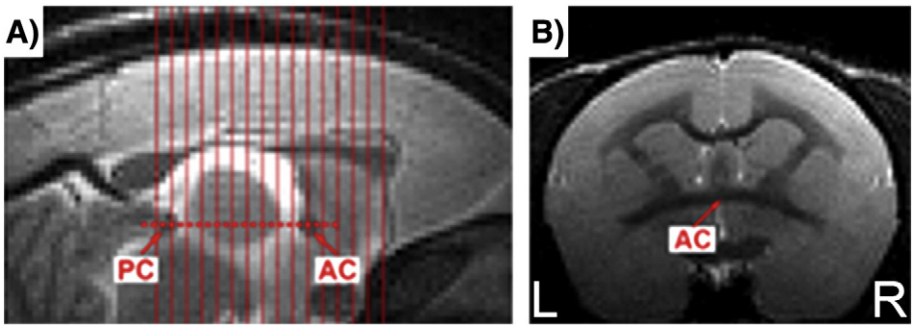

Fig. 1. Illustration of slice profiles used in functional MRI. (A) Sagittal plane through midline showing anterior (AC) and posterior (PC) commissures. Sixteen coronal slices, each 750 μm thick, were prescribed orthogonal to AC–PC line. (B) One of the coronal slices cutting across AC. R = right side; L = left side.

consistently by recognizing anatomical features, specifically the characteristic structures of white matter underneath SI and SII. Thus, SI and SII regions were also demarcated manually, in fixed shapes, based on the anatomical features shown in EPI images. The significance-defined and the fixed-shape regions gave similar results, and results from the latter were shown. For thalamus and caudate, however, only significance-defined regions were used, as the surrounding anatomical features were not salient enough for manual demarcation.

Amplitude and time-to-peak of stimulus-evoked response were estimated from the 40 s long fMRI time courses averaged across all trials of the same stimulus frequency in each session by fitting the fMRI signal to a Gamma function y(t) with 3 free parameters (A, τ, n) convolved with a 4-s boxcar (representing 4 s stimulus duration):

$$y(t) = [\Pi(t,0) - \Pi(t,4)] \otimes \left[A(t/\tau)^n \exp(-t/\tau)\Pi(t,0)\right], \quad (1)$$

where $\Pi(t,t_0) = 1$ if $t \geq t_0$ or $= 0$ if $t < t_0$, $\otimes$ represents convolution, and t is time (stimulus onset at $t = 0$). This model yielded estimations of response peak amplitude, time-to-peak (TTP) and full-width-at-half-maximum (FWHM) of y(t) with a higher temporal precision than the sampling time resolution.

Spontaneous functional connectivity

A few EPI scans without stimuli were conducted in each fMRI session. From each 800 s long scan, spontaneous functional connectivity between a pair of anatomical regions (as demarcated above) was measured by the correlation coefficient between the pair of time series. To construct a spontaneous functional connectivity map, one anatomical region was used as seed region, and the correlation coefficient between its time series and the time series of each voxel was computed. The calculations of correlation coefficient were also repeated with all time series filtered by a band-pass frequency filter (0.025 to 0.10 Hz). We analyzed the connectivity between the SI and SII regions within the same hemisphere. In addition, we also analyzed the interhemispheric connectivity between SI in left and right hemispheres [SI(L)–SI(R)], and between SII in left and right hemispheres [SII(L)–SII(R)].

Results

In total, 36 fMRI sessions were acquired in the present study. Mild electrical stimulation of the median nerve was delivered in a pseudo-randomized sequence of trials with different stimulus frequencies (see Materials and methods). In the awake experiments, each of the six trained animals was tested in two awake fMRI sessions separated by at least 7 days. Unilateral stimulation of either the left or right arm was counterbalanced across sessions, with no noticeable difference between the two. In the anesthetized experiments, each of the twelve animals was tested twice, once with each of the two anesthetic regimens, and separated by at least 30 days. Stimulation was only applied to the left arm. Throughout the fMRI experiments, both awake and anesthetized animals were monitored with an MR-compatible camera (MRC Systems, Heidelberg, Germany). No noticeable signs of stress were observed from any of the animals, with the awake animals appearing calm and relaxed throughout the examinations.

Stimulus-evoked fMRI responses in the awake versus anesthetized marmoset

Fig. 2 shows functional maps of the BOLD response evoked by electrical stimulation of the left forearm in representative sessions under each of the 3 anesthetic conditions. In awake subjects (Fig. 2A), unilateral electrical stimulation of the forearm evoked robust fMRI responses in the brain in regions throughout the somatosensory pathway, including thalamus and somatosensory cortex (SI and SII), as well as the dorsal striatum (caudate). In all identified regions, the fMRI responses were significant in both contralateral and ipsilateral sides, though contralateral responses had higher significance (F-value) than ipsilateral responses. Of all the identified regions throughout the somatosensory pathway, SI and SII displayed the largest F-values (Fig. 2A). On the other hand, both Low-P (Fig. 2B) and High-P (Fig. 2C) anesthesia regimens caused a substantial attenuation of the significance (F-value) of the responses in all regions (Figs. 2B–C). In particular, whereas the overall location and size of the functional SI and SII regions were preserved, responses in ipsilateral thalamus were difficult to detect under anesthesia (Figs. 2B–C), and responses in the caudate nucleus were abolished. Both in awake and anesthetized marmosets, only positive BOLD responses to the somatosensory stimulation were detected, and no significant negative responses were found in any of the regions covered by the RF coil array.

Differences between the fMRI responses obtained from awake and anesthetized marmosets can be seen more clearly in Fig. 3, which shows the BOLD response amplitudes averaged across all sessions in six regions of interest as a function of stimulation frequency. The awake

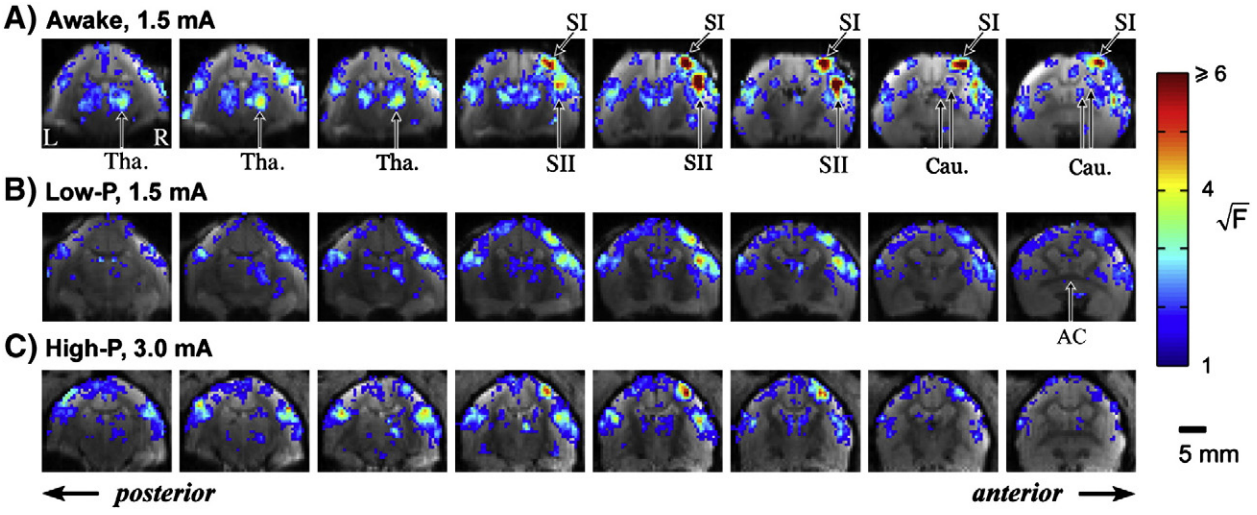

Fig. 2. Functional maps of the BOLD response evoked by electrical stimulation of the left forearm. Eight contiguous coronal slices immediately posterior to the anterior commissure (AC) are shown in representative sessions under each of the 3 anesthetic conditions: awake (A), low-propofol + fentanyl (Low-P, B) and high-propofol (High-P, C). Statistical significance of the stimulus-evoked response at all stimulation frequencies was measured by F-values derived from ANOVA, and the significance map was thresholded at a level correspondent to $P < 10^{-4}$ (see Materials and methods). Thalamus (Tha.), Caudate (Cau.), SI and SII regions were identified using anatomical landmarks including AC and the lateral sulcus (masked by SII responses), and these regions showed predominantly contralateral responses that were stronger in awake than in anesthetized sessions. R = right side; L = left side.

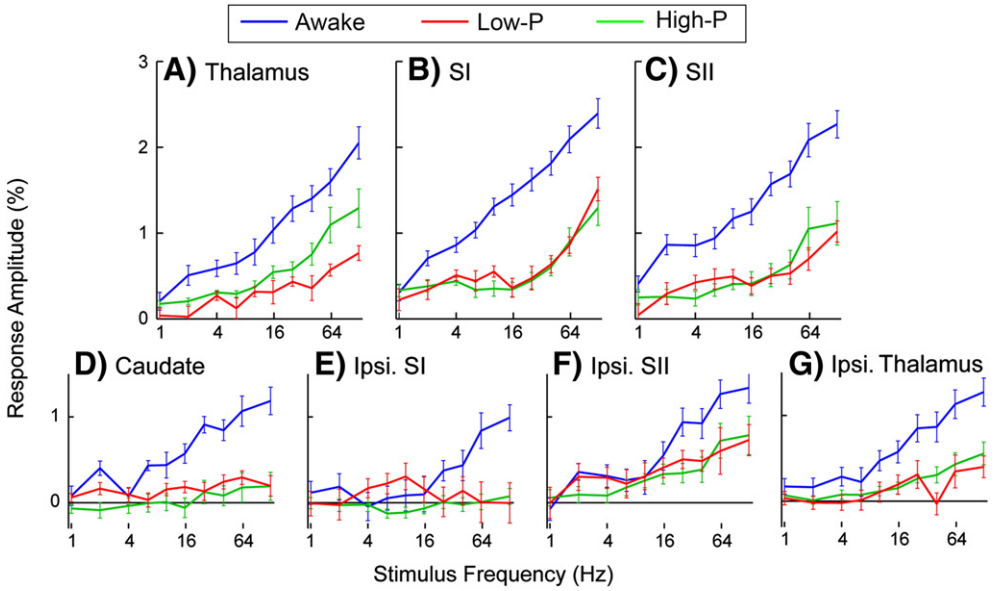

Fig. 3. Relationship of stimulus-evoked response amplitude with stimulus temporal frequency in 4 contralateral (A–D) and 3 ipsilateral (E–G) brain regions under awake (blue), low-propofol + fentanyl (red) and high-propofol (green) anesthesia. Error bars represent ±S.E.M. across all sessions (n = 12) obtained under each of the 3 anesthetic conditions. The current intensity of electrical stimulation was 1.5 mA in awake and low-propofol + fentanyl (Low-P) sessions, and 3.0 mA in high-propofol (High-P) sessions.

condition (blue) is compared with the two anesthetic conditions (green and red). Regions are contralateral to the stimulus unless noted otherwise. The amplitude of the fMRI response in conscious animals was in all cases stronger than in anesthetized animals. Note that this was true even though the current amplitude was doubled in the High-P regimen (see Materials and methods). In awake marmosets, responses in contralateral thalamus, SI, SII and caudate all increased monotonically with stimulus frequencies, and their amplitude data fit well to linearly proportional relationships with the logarithm of frequency across 1–128 Hz [e.g. SI $\text{amplitude}_{\text{awake}} = 0.35 \times \log(\text{frequency}) + 0.37\%$, residual standard deviation = 0.11%]. On the other hand, response amplitudes in ipsilateral thalamus, SI and SII regions of awake animals deviated from this linear relationship, remaining low and relatively constant below 16 Hz. As well, under anesthesia, response amplitudes in all regions were almost undetectable at low frequencies, but increased monotonically with stimulus frequency for frequencies above 16 Hz, with the exception of caudate and ipsilateral SI, regions in which anesthesia eliminated stimulus-evoked responses entirely.

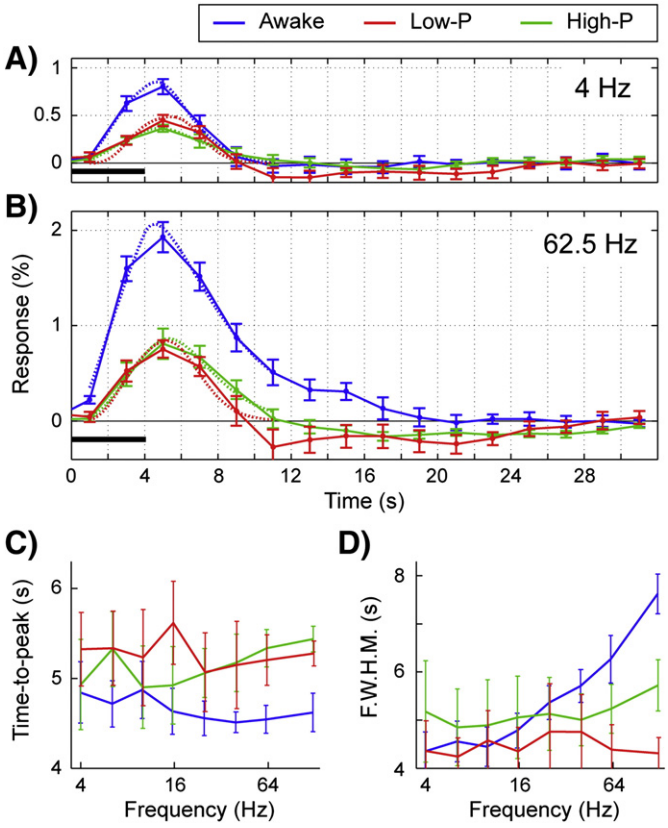

Fig. 4. Time-series and temporal parametric values of stimulus-evoked responses in SI. Evoked responses (solid lines) and Gamma function fits (dotted lines) are shown for 4 Hz (A) and 62.5 Hz (B) stimulations that last from 0 s to 4 s (horizontal black bars). Error bars: ±S.E.M. across all sessions (n = 12). Based on the Gamma function fits, response time-to-peak values (C), and full-width-at-half-maximum (FWHM) (D), are estimated and shown in relation to stimulus frequency. Error bars: ±S.E.M. estimated using bootstrapping with replacement method across all sessions.

In addition to showing higher response amplitude, awake animals also presented faster temporal dynamics of stimulus-evoked responses. Figs. 4A–B show the stimulus-evoked fMRI responses in SI to a 4 s-long stimulus period played at 4 Hz (Fig. 4A) and 62.5 Hz (Fig. 4B), respectively, averaged across animals. The time-to-peak (TTP) of the BOLD response in SI was significantly shorter (by circa 0.5 s) in awake than in anesthetized animals (Fig. 4C), indicating faster rise of the BOLD response to higher amplitudes in awake animals. Interestingly, unlike the monotonically increasing response amplitudes shown in Fig. 3, there was no dependence of TTP on stimulus frequency for any of the three preparations (Fig. 4C), indicating that TTP is dependent mostly on stimulus duration and suggesting increasing rates of growth of the fMRI responses with increasing frequencies. On the other hand, the full-width-at-half-maximum (FWHM) of the response in SI in awake – but not in anesthetized subjects – increased monotonically with stimulus frequency (Fig. 4D), becoming longer than the FWHM of anesthetized animals at high stimulus frequencies (≥20 Hz). Another noteworthy difference between the fMRI responses from awake and anesthetized animals was a small but detectable post-stimulus undershoot present only in anesthetized animals (Figs. 4A–B).

Spontaneous functional connectivity

To gauge the functional interdependence between the responsive areas identified above, we measured the spontaneous functional

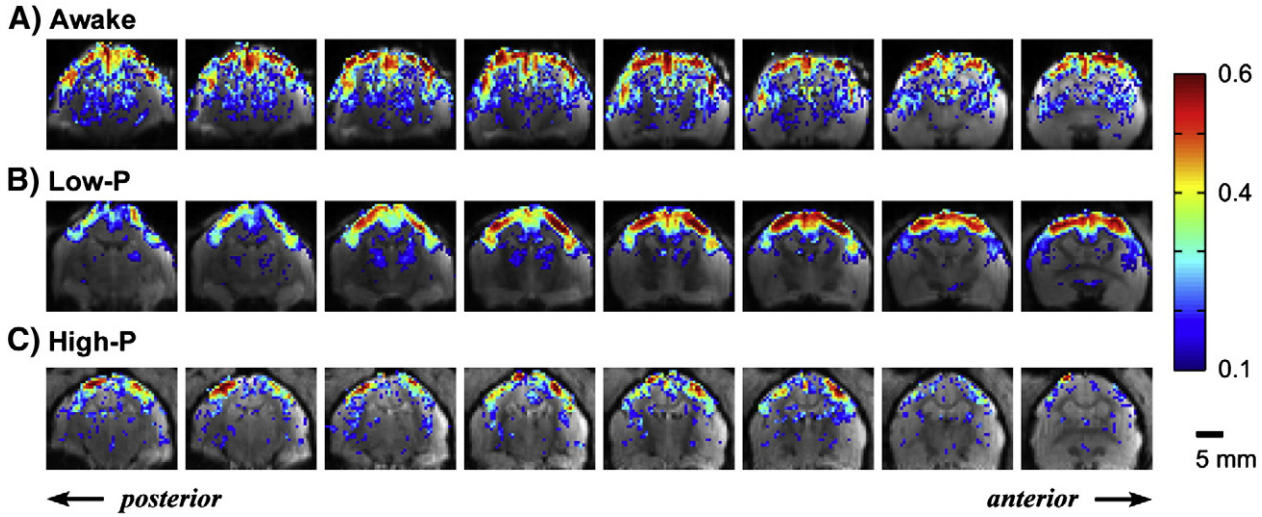

Fig. 5. Maps of spontaneous functional connectivity to a seed region in right SI, under awake and anesthetized conditions. Each map shows the correlation coefficient between time series of each pixel and time series of the seed region. The same 3 representative sessions as in Fig. 2 are shown, with scale between 0.1 and 0.6 (see colorbar). An arrow in each middle panel marks right SII, which shows high connectivity to right SI (bright colors) in awake (A) and low-propofol + fentanyl (Low-P, B), but low connectivity (blue) in high-propofol (High-P, C) anesthesia.

connectivity, defined as the correlation between fMRI fluctuations, in a pair of regions during scans with no stimulus presented. Fig. 5 shows representative connectivity maps obtained by using the SI region in one hemisphere as a seed region. In awake monkeys, there was a strong correlation with the homologous SI in the opposite hemisphere, as well as with the SII in both hemispheres. The correlation of SI with thalamus was significantly weaker, however, in agreement with previous findings in humans (Mhuircheartaigh et al., 2010; Zhang et al., 2008).

The connectivity within somatosensory cortex in both hemispheres was largely preserved under both anesthetic regimens, with one significant exception: the interareal SI–SII connectivity was significantly reduced by the High-P, but not by the Low-P regimen. Interhemispheric connectivities in SI and in SII were not affected by either regimen of anesthesia. These observations were quantified across all subjects (Fig. 6).

Discussion

Here we present the first experiments using high-resolution fMRI to measure somatosensory responses in conscious, awake marmosets. We were able to successfully acclimatize the animals to being comfortably restrained in the magnet. Robust and reproducible fMRI responses were obtained from conscious animals in contralateral and ipsilateral regions of the thalamus, primary (SI) and secondary (SII) somatosensory cortices, and the caudate nucleus. All regions showed a monotonic increase in the amplitude of the BOLD response with stimulus frequency. We compared BOLD responses in awake marmosets to those obtained in animals anesthetized under two different regimens of propofol anesthesia using the same stimulation paradigm. Anesthesia significantly attenuated responses in thalamus, SI, SII and ipsilateral SII and abolished responses in caudate and ipsilateral SI. Awake marmosets presented a faster rise and shorter TTP of the BOLD response to higher amplitudes. In addition, there was no dependence of TTP on stimulus frequency, suggesting increasing rates of growth of the fMRI responses with increasing frequencies. These results underscore the value of the conscious, awake marmoset preparation as an experimental model to study physiological responses in the somatosensory pathway, in the absence of anesthesia, so that the data can be compared most directly to fMRI in conscious humans.

fMRI in awake marmosets

The experimental use of non-human primates is an important step towards understanding processes in the highly evolved human brain. While several labs are now able to perform fMRI studies in alert old world monkeys, such as macaques (Andersen et al., 2002; Gamlin et al., 2006; Goense et al., 2010; Joseph et al., 2006; Keliris et al., 2007; Logothetis et al., 1999; Murnane and Howell, 2010; Pfeuffer et al., 2007), there have been only a handful of studies performed with marmosets (Brevard et al., 2006; Ferris et al., 2001, 2004; Meyer et al.,

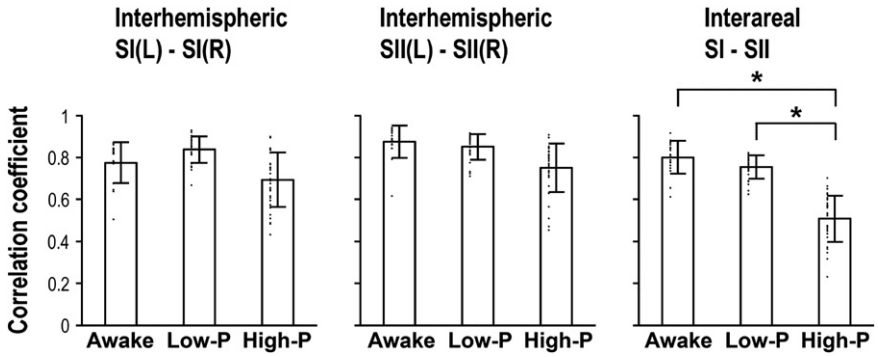

Fig. 6. Spontaneous functional connectivity between the two SI regions and between the two SII regions, and between the SI–SII regions, under awake, low-propofol + fentanyl (Low-P) and high-propofol (High-P) anesthesia. Each dot represents correlation coefficient computed from one scan without stimulus (800 s). Error bars: 1 Std. Dev. across scans. Stars denote significant differences ($P < 0.001$, Wilcoxon test).

2006; Tenney et al., 2004). The marmoset is becoming an increasingly important model in neuroscience, neurophysiology and neuropathology (Mansfield, 2003; Okano et al., 2012). It is a new world non-human primate with the same body weight as the rat, but with a relative brain size equivalent to the relative brain size of humans and approximately eight times larger than the rat brain (Marshall and Ridley, 2003). The marmoset's relatively large brain shares many aspects of neural anatomy found in more commonly studied primates, such as rhesus monkeys, including a large and well-developed cerebral cortex and cerebellum. The recent development of transgenic marmosets only adds to the attractiveness of this species to biomedical research (Sasaki et al., 2009). Previous fMRI studies in conscious marmosets have resorted to securing the animals to an MRI-compatible stereotaxic head holder by means of ear pieces and a bite bar after using a reversible, short-acting anesthetic to sedate the animals (Brevard et al., 2006; Ferris et al., 2001, 2004). As with several other fMRI studies in conscious, awake animals, we initiated the present work by restraining the animals by clamping surgically implanted head posts to a specially designed frame (Goense et al., 2010). While this approach allows maximum restraint of the animals, it brings in many disadvantages, including but not limited to the generation of susceptibility artifacts by the head implant that degrade image quality and the requirement for constant aseptic cleaning of the implant to prevent infections. In addition, the use of a head implant limits the use of the animal in longitudinal studies and significantly detracts from the major advantage of MRI as a noninvasive technique. In the course of the present work, we were able to develop a completely non-invasive, custom-fit helmet restraint that matches the contour of each individual head exactly, providing a comfortable, yet effective restraint that eliminated the use of headposts (Silva et al., 2011). The data obtained here from awake marmosets proved robust and highly reproducible. Awake animals provided fMRI responses in ipsilateral and contralateral regions of the thalamus, primary and secondary somatosensory cortices, and dorsal striatum. The responses increased monotonically with stimulus frequency, and had shorter times-to-peak than those obtained under identical conditions from anesthetized animals. The significance of these results is discussed in detail below.

Regions showing fMRI responses to somatosensory stimulation in marmosets

In awake marmosets, unilateral electrical stimulation of the forearm evoked robust fMRI responses in both ipsilateral and contralateral regions of the thalamus, SI, SII and caudate. While the surface coil array used did not provide enough coverage and sensitivity for detecting activation of the posterior parts of the brain, including cerebellum, the areas of activation agree well with the expected organization of the somatosensory pathway in marmosets (Kaas, 1993; Krubitzer and Kaas, 1990, 1992) and are in general agreement with human fMRI data (Backes et al., 2000; Groschel et al., 2013; Kampe et al., 2000; Klingner et al., 2011; Schafer et al., 2012). In marmosets, the thalamus projects densely to both SI and SII regions (Krubitzer and Kaas, 1992), forming a parallel organization of thalamocortical connections (Zhang et al., 1996). The bilateral activation of SI and SII reported here has also been obtained in humans undergoing electrical stimulation of the median nerve (Groschel et al., 2013; Klingner et al., 2011; Schafer et al., 2012), with the important difference that ipsilateral activation of SI in humans is usually negative rather than positive. Reasons for this are not entirely clear, but could be due to the different stimulation parameters and/or species differences. Human fMRI studies of the somatosensory pathway usually employ high currents that are individually adjusted to the level of the motor threshold, while we employed subthreshold currents. Interestingly, marmosets showed robust ipsilateral activation of the thalamus (Fig. 3G), which resembled significantly the activation of ipsilateral SII (Fig. 3F). Most animal and human fMRI studies fail to detect ipsilateral thalamic activity. However, Groschel et al reported negative ipsilateral thalamic activity together with negative ipsilateral SI and positive ipsilateral SII responses to median nerve stimulation (40 Hz) in humans (Groschel et al., 2013). It is well known that both SI and SII project back to the ipsilateral thalamus through reciprocal connections (Iyengar et al., 2007; Krubitzer and Kaas, 1992; Qi et al., 2002), and that thalamic activity may be modulated by these corticothalamic inputs (Theyel et al., 2010). Thus, it is possible that the observed ipsilateral thalamic activation results from feedback activation of ipsilateral SI, SII or, most likely, both. Further studies are necessary to elucidate this finding.

Effects of anesthesia on evoked response magnitude

The stimulus-evoked fMRI responses were stronger in awake animals than in animals under either the low-propofol + fentanyl (Low-P) or the high-propofol (High-P) anesthesia. Note that the Low-P anesthesia used here is akin to the idea of balanced anesthesia in clinical practice, as a low dose of fentanyl substantially reduces the minimum propofol dose required to maintain marmoset immobility during fMRI. In clinical settings, alfentanil lowers the propofol dose required to reach the same endpoints (Pavlin et al., 1999). However, the High-P regimen induced a stronger suppression of the sensory stimulus, requiring twice the current intensity (3.0 mA) in order to evoke the same SI and SII response amplitudes as under the Low-P condition. This agrees with the reported suppression of somatosensory cortical evoked potentials by propofol but not by remifentanil (Logginidou et al., 2003), and reflects the fact that fentanyl, in line with its analgesic rather than anesthetic role, elicits little suppression of the stimulus-evoked response amplitude. Since the dose of propofol is higher in the High-P regimen, this is also in line with a recent review on the effect of the dose of propofol on the responses to somatosensory stimulation in cortex and thalamus (Fiset et al., 2005).

Both regimens of anesthesia abolished responses in ipsilateral SI and caudate, but not ipsilateral SII. Assuming that anesthetic effects accumulate and become stronger with more synaptic connections, this result may suggest that ipsilateral SII response is driven by direct corticocortical connections from (contralateral) SII (Klingner et al., 2012), whereas ipsilateral SI and caudate show responses that are not driven by such direct connections. This result is consistent with neuronal tracing studies in marmosets, where direct interhemispheric projections between the two SIs are sparse and often miss the SI representations of hands, but direct interhemispheric projections between the two SIIs are rich (Krubitzer and Kaas, 1990). However, the ipsilateral SI response to electrical stimulation of the forearm has been observed in macaques under isoflurane anesthesia (Lipton et al., 2006), and has also been observed in rats under halothane, but not under α-chloralose anesthesia (Shulman et al., 2009), suggesting that the anesthesia-induced abolishment of ipsilateral SI response is, like the anesthetic effect on contralateral SI, dependent on the choice of anesthetic agent.

Stimulation frequency dependence

Previous electrophysiological studies in marmosets have shown robust activation of mechanoreceptive afferent fibers (Coleman et al., 2001) as well as thalamocortical neurons projecting to SI and to SII in response to stimulation rates of up to 600 Hz (Zhang et al., 2001a). Due to technical limitations of our equipment, we were not able to stimulate the marmosets with frequencies higher than 128 Hz. Nonetheless, the monotonic relationship of the BOLD response to stimulus frequency observed in awake marmosets is in good agreement with those previous electrophysiological studies in marmosets, and with a recent optical imaging study in awake rats (Martin et al., 2006). To better characterize the frequency dependence of the BOLD response in the somatosensory pathway of awake marmosets, it will be interesting in future studies to extend the range of stimulation frequencies further. In the present

work, there were two somewhat surprising findings from the experiments in anesthetized marmosets. First, the absence of significant responses at low frequencies observed here under propofol anesthesia deviates significantly from what would be expected based on rat experiments. Under anesthesia, fMRI responses in the rat somatosensory cortex show a tight tuning curve with optimal frequencies around 3 Hz under α-chloralose (Silva et al., 1999), 9 Hz under urethane (Huttunen et al., 2008) or 12 Hz under isoflurane (Masamoto et al., 2007). Robust fMRI responses to 10 Hz stimulation were recently reported in propofol anesthetized rats (Griffin et al., 2010). Thus, anesthetics alter the physiological responses to different frequencies, and in a manner that is idiosyncratic to each anesthetic agent. The second surprising observation was the increase in the amplitude of the BOLD response in anesthetized animals for frequencies >16 Hz, which would not be expected based on previous work. One possibility for this difference is that previous studies in rats only measured frequencies up to 20 Hz, and they may have simply missed the relevant frequency range, which was somewhat higher. Another possibility for the discrepancy is that propofol has fundamentally different effects than the anesthetics previously used to address this question in rats. A third possibility is that marmosets, as primates with a highly adapted forelimb and hand, have an inherently higher sensitivity to somatosensory stimulation, which is also more robust against anesthetic suppression. In a similar vein, it is interesting to speculate that there may be other thalamocortical pathways that bypass primary and secondary sensory cortices and that have a different sensitivity to anesthesia than the primary thalamocortical pathways. The main purpose of these alternate pathways is to provide a fast and efficient way for transmitting information to multimodal cortical areas, to allow early detection of salient events and trigger immediate and appropriate behavior (Liang et al., 2012). This possibility warrants further investigation.

Anesthesia effects on hemodynamic response function

At any of the tested frequencies, the BOLD response in awake marmosets had higher amplitude, shorter onset-times (not shown) and shorter TTP than anesthetized monkeys (Fig. 4), implying that anesthesia probably interferes with the synthesis and release of vasoactive agents, and possibly with the vascular response, turning the hemodynamic response sluggish. Reports of significantly delayed hemodynamic responses due to different anesthetics have been made both in animals (Franceschini et al., 2010; Huttunen et al., 2008; Martin et al., 2006) and humans (Qiu et al., 2008). Interestingly, in spite of their shorter TTP, awake marmosets presented longer FWHM of the BOLD responses at high stimulus frequencies than anesthetized monkeys. This can be explained by a larger involvement of the local vasculature in the spatiotemporal evolution of the response under awake conditions. A possible model is that the functional neuronal circuitry in the awake state elicits faster synthesis and release of vasoactive agents over a wider area, so that more cells participate in neurovascular coupling in the awake state than in the anesthetized state. This higher number of active cells would produce a larger amount and faster release of vasodilatatory agents at the onset of neural activity, leading to shorter onset times and TTP, but to larger amplitudes. Upon cessation of the neural activity, the larger additional functional volume of blood would take longer to be drained away, suffering more dispersive effects in the venous side of the vasculature (Hirano et al., 2011; Silva et al., 2007), leading to longer FWHM in awake than in anesthetized animals. Taken together, the present data suggest that anesthesia affects neural activity and neurovascular coupling in complex ways.

Anesthesia and functional connectivity

Many studies have shown that anesthesia reduces the resting-state, or spontaneous, functional connectivity in a manner that is often specific to brain regions and anesthetic agents (Alkire, 2008). In particular, a recent fMRI study in human reports that spontaneous functional connectivity between putamen and cortex is reduced by propofol anesthesia, but the connectivity between thalamus and cortex is not (Mhuircheartaigh et al., 2010). Here we report that effects of propofol on spontaneous functional connectivity within the somatosensory cortex are also region-specific. Connectivity between SI and SII in a hemisphere is reduced under the high-propofol regimen, but connectivity between SI in two hemispheres, and between SII in two hemispheres are not reduced. Interestingly, the connectivity between SI in two hemispheres has been found to be reduced by sevoflurane in humans (Peltier et al., 2005) and by α-chloralose in rats (Lu et al., 2007), suggesting that the anesthesia-induced suppression of interhemispheric functional connectivity is, like the anesthetic effect on stimulus-evoked responses, dependent on the choice of anesthetic agent. Furthermore, spontaneous SI–SII functional connectivity does not reduce under the low-propofol anesthetic regime, which constitutes a mixture of low-dose propofol and fentanyl. This may be a combination of two factors: that the effect of propofol may be dose-dependent (Alkire, 2008), and that fentanyl may enhance spontaneous functional connectivity. The latter is supported by findings that spontaneous functional connectivity is increased by various analgesic mechanisms that involve opioid receptors in central sensorimotor network, including acupuncture (Dhond et al., 2008), hypnosis (Faymonville et al., 2003), and placebo effect (Wager et al., 2007).

Acknowledgments

We thank Xianfeng (Lisa) Zhang, Julie Mackel, Peter Minnig and Dr. James O'Malley for their invaluable help in animal preparation. We also thank Dr. Brian Wandell and his colleagues at Stanford University for providing the mrVista software on their website. This research was supported by the Intramural Research Program of the NINDS, National Institutes of Health.

Conflict of interest

The authors have no conflicts of interest to declare with regard to the subject matter of the present research.

References

Alkire, M.T., 2008. Loss of effective connectivity during general anesthesia. Int. Anesthesiol. Clin. 46, 55–73.
Andersen, A.H., Zhang, Z., Barber, T., Rayens, W.S., Zhang, J., Grondin, R., Hardy, P., Gerhardt, G.A., Gash, D.M., 2002. Functional MRI studies in awake rhesus monkeys: methodological and analytical strategies. J. Neurosci. Methods 118, 141–152.
Attwell, D., Iadecola, C., 2002. The neural basis of functional brain imaging signals. Trends Neurosci. 25, 621–625.
Backes, W.H., Mess, W.H., van Kranen-Mastenbroek, V., Reulen, J.P., 2000. Somatosensory cortex responses to median nerve stimulation: fMRI effects of current amplitude and selective attention. Clin. Neurophysiol. 111, 1738–1744.
Bandettini, P.A., 2012. Twenty years of functional MRI: the science and the stories. Neuroimage 62, 575–588.
Bendor, D., Wang, X., 2005. The neuronal representation of pitch in primate auditory cortex. Nature 436, 1161–1165.
Bock, N.A., Kocharyan, A., Liu, J.V., Silva, A.C., 2009. Visualizing the entire cortical myelination pattern in marmosets with magnetic resonance imaging. J. Neurosci. Methods 185, 15–22.
Bock, N.A., Hashim, E., Kocharyan, A., Silva, A.C., 2011. Visualizing myeloarchitecture with magnetic resonance imaging in primates. Ann. N. Y. Acad. Sci. 1225 (Suppl. 1), E171–E181.
Bourne, J.A., Rosa, M.G., 2006. Hierarchical development of the primate visual cortex, as revealed by neurofilament immunoreactivity: early maturation of the middle temporal area (MT). Cereb. Cortex 16, 405–414.
Brevard, M.E., Meyer, J.S., Harder, J.A., Ferris, C.F., 2006. Imaging brain activity in conscious monkeys following oral MDMA ("ecstasy"). Magn. Reson. Imaging 24, 707–714.
Clare, S., Humberstone, M., Hykin, J., Blumhardt, L.D., Bowtell, R., Morris, P., 1999. Detecting activations in event-related fMRI using analysis of variance. Magn. Reson. Med. 42, 1117–1122.
Coleman, G.T., Bahramali, H., Zhang, H.Q., Rowe, M.J., 2001. Characterization of tactile afferent fibers in the hand of the marmoset monkey. J. Neurophysiol. 85, 1793–1804.

de la Mothe, L.A., Blumell, S., Kajikawa, Y., Hackett, T.A., 2006. Thalamic connections of the auditory cortex in marmoset monkeys: core and medial belt regions. J. Comp. Neurol. 496, 72–96.
de la Mothe, L.A., Blumell, S., Kajikawa, Y., Hackett, T.A., 2012a. Cortical connections of auditory cortex in marmoset monkeys: lateral belt and parabelt regions. Anat. Rec. (Hoboken) 295, 800–821.
de la Mothe, L.A., Blumell, S., Kajikawa, Y., Hackett, T.A., 2012b. Thalamic connections of auditory cortex in marmoset monkeys: lateral belt and parabelt regions. Anat. Rec. (Hoboken) 295, 822–836.
Dhond, R.P., Yeh, C., Park, K., Kettner, N., Napadow, V., 2008. Acupuncture modulates resting state connectivity in default and sensorimotor brain networks. Pain 136, 407–418.
Dubowitz, D.J., Chen, D.Y., Atkinson, D.J., Scadeng, M., Martinez, A., Andersen, M.B., Andersen, R.A., Bradley Jr., W.G., 2001. Direct comparison of visual cortex activation in human and non-human primates using functional magnetic resonance imaging. J. Neurosci. Methods 107, 71–80.
Faymonville, M.E., Roediger, L., Del Fiore, G., Delgueldre, C., Phillips, C., Lamy, M., Luxen, A., Maquet, P., Laureys, S., 2003. Increased cerebral functional connectivity underlying the antinociceptive effects of hypnosis. Brain Res. Cogn. Brain Res. 17, 255–262.
Ferris, C.F., Snowdon, C.T., King, J.A., Duong, T.Q., Ziegler, T.E., Ugurbil, K., Ludwig, R., Schultz-Darken, N.J., Wu, Z., Olson, D.P., Sullivan Jr., J.M., Tannenbaum, P.L., Vaughan, J.T., 2001. Functional imaging of brain activity in conscious monkeys responding to sexually arousing cues. Neuroreport 12, 2231–2236.
Ferris, C.F., Snowdon, C.T., King, J.A., Sullivan Jr., J.M., Ziegler, T.E., Olson, D.P., Schultz-Darken, N.J., Tannenbaum, P.L., Ludwig, R., Wu, Z., Einspanier, A., Vaughan, J.T., Duong, T.Q., 2004. Activation of neural pathways associated with sexual arousal in non-human primates. J. Magn. Reson. Imaging 19, 168–175.
Fiset, P., Plourde, G., Backman, S.B., 2005. Brain imaging in research on anesthetic mechanisms: studies with propofol. Prog. Brain Res. 150, 245–250.
Franceschini, M.A., Radhakrishnan, H., Thakur, K., Wu, W., Ruvinskaya, S., Carp, S., Boas, D.A., 2010. The effect of different anesthetics on neurovascular coupling. Neuroimage 51, 1367–1377.
Gamlin, P.D., Ward, M.K., Bolding, M.S., Grossmann, J.K., Twieg, D.B., 2006. Developing functional magnetic resonance imaging techniques for alert macaque monkeys. Methods 38, 210–220.
Goense, J.B., Whittingstall, K., Logothetis, N.K., 2010. Functional magnetic resonance imaging of awake behaving macaques. Methods 50, 178–188.
Griffin, K.M., Blau, C.W., Kelly, M.E., O'Herlihy, C., O'Connell, P.R., Jones, J.F., Kerskens, C.M., 2010. Propofol allows precise quantitative arterial spin labelling functional magnetic resonance imaging in the rat. Neuroimage 51, 1395–1404.
Groschel, S., Sohns, J.M., Schmidt-Samoa, C., Baudewig, J., Becker, L., Dechent, P., Kastrup, A., 2013. Effects of age on negative BOLD signal changes in the primary somatosensory cortex. Neuroimage 71C, 10–18.
Hirano, Y., Stefanovic, B., Silva, A.C., 2011. Spatiotemporal evolution of the functional magnetic resonance imaging response to ultrashort stimuli. J. Neurosci. 31, 1440–1447.
Huttunen, J.K., Grohn, O., Penttonen, M., 2008. Coupling between simultaneously recorded BOLD response and neuronal activity in the rat somatosensory cortex. Neuroimage 39, 775–785.
Iyengar, S., Qi, H.X., Jain, N., Kaas, J.H., 2007. Cortical and thalamic connections of the representations of the teeth and tongue in somatosensory cortex of new world monkeys. J. Comp. Neurol. 501, 95–120.
Joseph, J.E., Powell, D.K., Andersen, A.H., Bhatt, R.S., Dunlap, M.K., Foldes, S.T., Forman, E., Hardy, P.A., Steinmetz, N.A., Zhang, Z., 2006. fMRI in alert, behaving monkeys: an adaptation of the human infant familiarization novelty preference procedure. J. Neurosci. Methods 157, 10–24.
Kaas, J.H., 1993. The functional organization of somatosensory cortex in primates. Ann. Anat. 175, 509–518.
Kampe, K.K., Jones, R.A., Auer, D.P., 2000. Frequency dependence of the functional MRI response after electrical median nerve stimulation. Hum. Brain Mapp. 9, 106–114.
Keliris, G.A., Shmuel, A., Ku, S.P., Pfeuffer, J., Oeltermann, A., Steudel, T., Logothetis, N.K., 2007. Robust controlled functional MRI in alert monkeys at high magnetic field: effects of jaw and body movements. Neuroimage 36, 550–570.
Klingner, C.M., Huonker, R., Flemming, S., Hasler, C., Brodoehl, S., Preul, C., Burmeister, H., Kastrup, A., Witte, O.W., 2011. Functional deactivations: multiple ipsilateral brain areas engaged in the processing of somatosensory information. Hum. Brain Mapp. 32, 127–140.
Klingner, C.M., Hasler, C., Brodoehl, S., Axer, H., Witte, O.W., 2012. Perceptual plasticity is mediated by connectivity changes of the medial thalamic nucleus. Hum. Brain Mapp. http://dx.doi.org/10.1002/hbm.22074.
Krubitzer, L.A., Kaas, J.H., 1990. The organization and connections of somatosensory cortex in marmosets. J. Neurosci. 10, 952–974.
Krubitzer, L.A., Kaas, J.H., 1992. The somatosensory thalamus of monkeys: cortical connections and a redefinition of nuclei in marmosets. J. Comp. Neurol. 319, 123–140.
Liang, M., Mouraux, A., Iannetti, G.D., 2012. Bypassing primary sensory cortices—a direct thalamocortical pathway for transmitting salient sensory information. Cereb. Cortex 23, 1–11.
Lipton, M.L., Fu, K.M., Branch, C.A., Schroeder, C.E., 2006. Ipsilateral hand input to area 3b revealed by converging hemodynamic and electrophysiological analyses in macaque monkeys. J. Neurosci. 26, 180–185.
Logginidou, H.G., Li, B.H., Li, D.P., Lohmann, J.S., Schuler, H.G., DiVittore, N.A., Kreiser, S., Cronin, A.J., 2003. Propofol suppresses the cortical somatosensory evoked potential in rats. Anesth. Analg. 97, 1784–1788.
Logothetis, N.K., 2008. What we can do and what we cannot do with fMRI. Nature 453, 869–878.
Logothetis, N.K., Guggenberger, H., Peled, S., Pauls, J., 1999. Functional imaging of the monkey brain. Nat. Neurosci. 2, 555–562.
Lu, H., Zuo, Y., Gu, H., Waltz, J.A., Zhan, W., Scholl, C.A., Rea, W., Yang, Y., Stein, E.A., 2007. Synchronized delta oscillations correlate with the resting-state functional MRI signal. Proc. Natl. Acad. Sci. U. S. A. 104, 18265–18269.
Maier, A., Wilke, M., Aura, C., Zhu, C., Ye, F.Q., Leopold, D.A., 2008. Divergence of fMRI and neural signals in V1 during perceptual suppression in the awake monkey. Nat. Neurosci. 11, 1193–1200.
Mansfield, K., 2003. Marmoset models commonly used in biomedical research. Comp. Med. 53, 383–392.
Marshall, J.W., Ridley, R.M., 2003. Assessment of cognitive and motor deficits in a marmoset model of stroke. ILAR J. 44, 153–160.
Martin, C., Martindale, J., Berwick, J., Mayhew, J., 2006. Investigating neural-hemodynamic coupling and the hemodynamic response function in the awake rat. Neuroimage 32, 33–48.
Masamoto, K., Kim, T., Fukuda, M., Wang, P., Kim, S.G., 2007. Relationship between neural, vascular, and BOLD signals in isoflurane-anesthetized rat somatosensory cortex. Cereb. Cortex 17, 942–950.
Meyer, J.S., Brevard, M.E., Piper, B.J., Ali, S.F., Ferris, C.F., 2006. Neural effects of MDMA as determined by functional magnetic resonance imaging and magnetic resonance spectroscopy in awake marmoset monkeys. Ann. N. Y. Acad. Sci. 1074, 365–376.
Mhuircheartaigh, R.N., Rosenorn-Lanng, D., Wise, R., Jbabdi, S., Rogers, R., Tracey, I., 2010. Cortical and subcortical connectivity changes during decreasing levels of consciousness in humans: a functional magnetic resonance imaging study using propofol. J. Neurosci. 30, 9095–9102.
Murnane, K.S., Howell, L.L., 2010. Development of an apparatus and methodology for conducting functional magnetic resonance imaging (fMRI) with pharmacological stimuli in conscious rhesus monkeys. J. Neurosci. Methods 191, 11–20.
Nakahara, K., Hayashi, T., Konishi, S., Miyashita, Y., 2002. Functional MRI of macaque monkeys performing a cognitive set-shifting task. Science 295, 1532–1536.
Nelissen, K., Vanduffel, W., 2011. Grasping-related functional magnetic resonance imaging brain responses in the macaque monkey. J. Neurosci. 31, 8220–8229.
Newman, J.D., Kenkel, W.M., Aronoff, E.C., Bock, N.A., Zametkin, M.R., Silva, A.C., 2009. A combined histological and MRI brain atlas of the common marmoset monkey, *Callithrix jacchus*. Brain Res. Rev. 62, 1–18.
Ogawa, S., Tank, D.W., Menon, R., Ellermann, J.M., Kim, S.G., Merkle, H., Ugurbil, K., 1992. Intrinsic signal changes accompanying sensory stimulation: functional brain mapping with magnetic resonance imaging. Proc. Natl. Acad. Sci. U. S. A. 89, 5951–5955.
Okano, H., Hikishima, K., Iriki, A., Sasaki, E., 2012. The common marmoset as a novel animal model system for biomedical and neuroscience research applications. Semin. Fetal Neonatal Med. 17, 336–340.
Palazzi, X., Bordier, N., 2008. The Marmoset Brain in Stereotaxic Coordinates. Springer, New York.
Pavlin, D.J., Arends, R.H., Gunn, H.C., Van Norman, G., Koerschgen, M.E., Shen, D.D., 1999. Optimal propofol–alfentanil combinations for supplementing nitrous oxide for outpatient surgery. Anesthesiology 91, 97–108.
Peltier, S.J., Kerssens, C., Hamann, S.B., Sebel, P.S., Byas-Smith, M., Hu, X., 2005. Functional connectivity changes with concentration of sevoflurane anesthesia. Neuroreport 16, 285–288.
Petkov, C.I., Kayser, C., Augath, M., Logothetis, N.K., 2006. Functional imaging reveals numerous fields in the monkey auditory cortex. PLoS Biol. 4, e215.
Pfeuffer, J., Shmuel, A., Keliris, G.A., Steudel, T., Merkle, H., Logothetis, N.K., 2007. Functional MR imaging in the awake monkey: effects of motion on dynamic off-resonance and processing strategies. Magn. Reson. Imaging 25, 869–882.
Philibert, B., Beitel, R.E., Nagarajan, S.S., Bonham, B.H., Schreiner, C.E., Cheung, S.W., 2005. Functional organization and hemispheric comparison of primary auditory cortex in the common marmoset (*Callithrix jacchus*). J. Comp. Neurol. 487, 391–406.
Qi, H.X., Lyon, D.C., Kaas, J.H., 2002. Cortical and thalamic connections of the parietal ventral somatosensory area in marmoset monkeys (*Callithrix jacchus*). J. Comp. Neurol. 443, 168–182.
Qiu, M., Ramani, R., Swetye, M., Rajeevan, N., Constable, R.T., 2008. Anesthetic effects on regional CBF, BOLD, and the coupling between task-induced changes in CBF and BOLD: an fMRI study in normal human subjects. Magn. Reson. Med. 60, 987–996.
Ress, D., Glover, G.H., Liu, J., Wandell, B., 2007. Laminar profiles of functional activity in the human brain. Neuroimage 34, 74–84.
Roberts, A.C., Tomic, D.L., Parkinson, C.H., Roeling, T.A., Cutter, D.J., Robbins, T.W., Everitt, B.J., 2007. Forebrain connectivity of the prefrontal cortex in the marmoset monkey (*Callithrix jacchus*): an anterograde and retrograde tract-tracing study. J. Comp. Neurol. 502, 86–112.
Sasaki, E., Suemizu, H., Shimada, A., Hanazawa, K., Oiwa, R., Kamioka, M., Tomioka, I., Sotomaru, Y., Hirakawa, R., Eto, T., Shiozawa, S., Maeda, T., Ito, M., Ito, R., Kito, C., Yagihashi, C., Kawai, K., Miyoshi, H., Tanioka, Y., Tamaoki, N., Habu, S., Okano, H., Nomura, T., 2009. Generation of transgenic non-human primates with germline transmission. Nature 459, 523–527.
Schafer, K., Blankenburg, F., Kupers, R., Gruner, J.M., Law, I., Lauritzen, M., Larsson, H.B., 2012. Negative BOLD signal changes in ipsilateral primary somatosensory cortex are associated with perfusion decreases and behavioral evidence for functional inhibition. Neuroimage 59, 3119–3127.
Schmid, M.C., Mrowka, S.W., Turchi, J., Saunders, R.C., Wilke, M., Peters, A.J., Ye, F.Q., Leopold, D.A., 2010. Blindsight depends on the lateral geniculate nucleus. Nature 466, 373–377.
Shulman, R.G., Hyder, F., Rothman, D.L., 2009. Baseline brain energy supports the state of consciousness. Proc. Natl. Acad. Sci. U. S. A. 106, 11096–11101.
Silva, A.C., Lee, S.P., Yang, G., Iadecola, C., Kim, S.G., 1999. Simultaneous blood oxygenation level-dependent and cerebral blood flow functional magnetic resonance imaging during forepaw stimulation in the rat. J. Cereb. Blood Flow Metab. 19, 871–879.

Silva, A.C., Koretsky, A.P., Duyn, J.H., 2007. Functional MRI impulse response for BOLD and CBV contrast in rat somatosensory cortex. Magn. Reson. Med. 57, 1110–1118.
Silva, A.C., Liu, J.V., Hirano, Y., Leoni, R.F., Merkle, H., Mackel, J.B., Zhang, X.F., Nascimento, G.C., Stefanovic, B., 2011. Longitudinal functional magnetic resonance imaging in animal models. Methods Mol. Biol. 711, 281–302.
Srihasam, K., Sullivan, K., Savage, T., Livingstone, M.S., 2010. Noninvasive functional MRI in alert monkeys. Neuroimage 51, 267–273.
Tenney, J.R., Marshall, P.C., King, J.A., Ferris, C.F., 2004. fMRI of generalized absence status epilepticus in conscious marmoset monkeys reveals corticothalamic activation. Epilepsia 45, 1240–1247.
Theyel, B.B., Llano, D.A., Sherman, S.M., 2010. The corticothalamocortical circuit drives higher-order cortex in the mouse. Nat. Neurosci. 13, 84–88.
Van der Linden, A., Van Camp, N., Ramos-Cabrer, P., Hoehn, M., 2007. Current status of functional MRI on small animals: application to physiology, pathophysiology, and cognition. NMR Biomed. 20, 522–545.
Wager, T.D., Scott, D.J., Zubieta, J.K., 2007. Placebo effects on human mu-opioid activity during pain. Proc. Natl. Acad. Sci. U. S. A. 104, 11056–11061.
Wilke, M., Mueller, K.M., Leopold, D.A., 2009. Neural activity in the visual thalamus reflects perceptual suppression. Proc. Natl. Acad. Sci. U. S. A. 106, 9465–9470.
Zhang, H.Q., Murray, G.M., Turman, A.B., Mackie, P.D., Coleman, G.T., Rowe, M.J., 1996. Parallel processing in cerebral cortex of the marmoset monkey: effect of reversible SI inactivation on tactile responses in SII. J. Neurophysiol. 76, 3633–3655.
Zhang, H.Q., Murray, G.M., Coleman, G.T., Turman, A.B., Zhang, S.P., Rowe, M.J., 2001a. Functional characteristics of the parallel SI- and SII-projecting neurons of the thalamic ventral posterior nucleus in the marmoset. J. Neurophysiol. 85, 1805–1822.
Zhang, H.Q., Zachariah, M.K., Coleman, G.T., Rowe, M.J., 2001b. Hierarchical equivalence of somatosensory areas I and II for tactile processing in the cerebral cortex of the marmoset monkey. J. Neurophysiol. 85, 1823–1835.
Zhang, D., Snyder, A.Z., Fox, M.D., Sansbury, M.W., Shimony, J.S., Raichle, M.E., 2008. Intrinsic functional relations between human cerebral cortex and thalamus. J. Neurophysiol. 100, 1740–1748.